NASA TECHNICAL NOTE

NASA TN D-3139

c. 1

NASA TN D-3139

MAGNETIC CONTROL OF THE FLOW OF HOT COMBUSTION GASES IN HYDROGEN-OXYGEN COMBUSTION AT 14 ATMOSPHERES

by Ronald Razner

Lewis Research Center

Cleveland, Ohio

NATIONAL AERONAUTICS AND SPACE ADMINISTRATION - WASHINGTON, D. C. - DECEMBER 1965

NASA TN D-3139

MAGNETIC CONTROL OF THE FLOW OF HOT COMBUSTION GASES IN HYDROGEN-OXYGEN COMBUSTION AT 14 ATMOSPHERES

By Ronald Razner

Lewis Research Center
Cleveland, Ohio

NATIONAL AERONAUTICS AND SPACE ADMINISTRATION

For sale by the Clearinghouse for Federal Scientific and Technical Information
Springfield, Virginia 22151 – Price $1.00

MAGNETIC CONTROL OF THE FLOW OF HOT COMBUSTION GASES IN HYDROGEN-OXYGEN COMBUSTION AT 14 ATMOSPHERES

by Ronald Razner

Lewis Research Center

SUMMARY

The feasibility of using electromagnetic forces for the purpose of directing the flow of hot combustion gases was investigated in the combustion of gaseous hydrogen and liquid oxygen at a pressure of 14 atmospheres.

Radiation between 2500 and 3500 angstroms emitted in the combustion process was used to detect changes in the extent of spreading of a single jet of liquid oxygen reacting in an atmosphere of gaseous hydrogen. This radiation is known to consist of hydroxyl radical and oxygen bands plus a continuum.

In general, the exertion of electromagnetic forces of a useful magnitude depended on the existence of a suitably high ion population in the combustion gases. When this population was sufficiently large, the velocity of the gases coupled with an externally applied magnetic field of 0.0200 to 0.0380 weber per square meter to exert an influence of practical magnitude on the directional flow of the gases.

Calculated estimates are made and discussed to compare the effectiveness of two methods for increasing the ion population in hot gases of a type encountered in hydrogen-oxygen combustion.

INTRODUCTION

A persistent problem in the design of chemical combustors involves the control of damage to mechanical surfaces resulting from contact with hot combustion gases. This problem increases in complexity with increasing temperature and pressure. Consequently, as a part of effective combustor design, investigating all possible methods of heat-transfer control is desirable.

To date the most serious heat-transfer problems known occur in a field quite far removed from chemical combustion. These problems are in areas of plasma physics con-

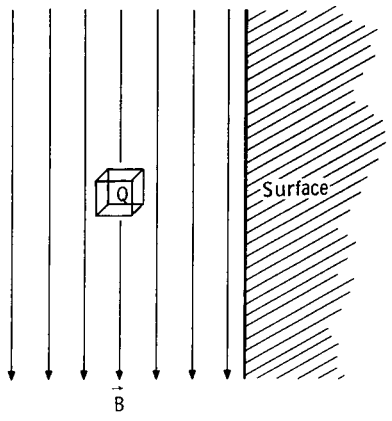

Figure 1. - Visualization of volume element of fluid in a flow stream with impressed magnetic field.

cerned with controlled thermonuclear fusion, where it is suggested that heat transfer can be controlled by means of magnetic confinement. In recent years extensive theoretical and experimental research has been done in this area.

While the physical conditions of high-pressure chemical combustion are quite different from those encountered in the physics of highly ionized and fully ionized plasmas, a consideration of the electrical properties of hot combustion gases (ref. 1) suggests that certain aspects of the principle of magnetic confinement might still be applied. The practicability of this concept would be established if it could be shown that directional flows can be significantly influenced by applied magnetic fields of reasonable intensity.

The basic problem is depicted schematically in figure 1. A volume element of combustible material Q near a mechanical surface is subject to a sudden expansion through the process of combustion. It is shown in appendix A that if the expanding gas has a sufficiently high electric conductivity, the presence of a magnetic field $\vec{B}$ parallel to the surface will set up forces that result in a preferred direction of gas expansion parallel to the surface. This effect increases as the electric conductivity increases.

The effect of an externally applied magnetic field on the expansion of a single jet of liquid oxygen burning in an atmosphere of gaseous hydrogen was studied at a pressure of 14 atmospheres in a rocket combustor. A provision was made for increasing the ion population in the combustor by using the moderate (initial) electric conductivity of the burning jet to support a small electric current discharge.

Spectral radiation of known origin (ref. 2) emitted in hydrogen-oxygen combustion was used photographically to detect and to study the desired effects. Since the radiation intensity increases as a function of temperature, any influence on the flow stream detected by using this radiation can be interpreted as an influence on the high-temperature portions of the gases.

An estimate was made of the lower limit of the ion population produced by an electric current flowing in the combustion gases. This limit is compared with calculated estimates of thermal ion populations produced by the technique of seeding.

APPARATUS AND PROCEDURE

The combustor (fig. 2) was constructed in sections consisting of an injector, boron nitride electrical insulators, magnetic coils, window section, and nozzle. All parts were

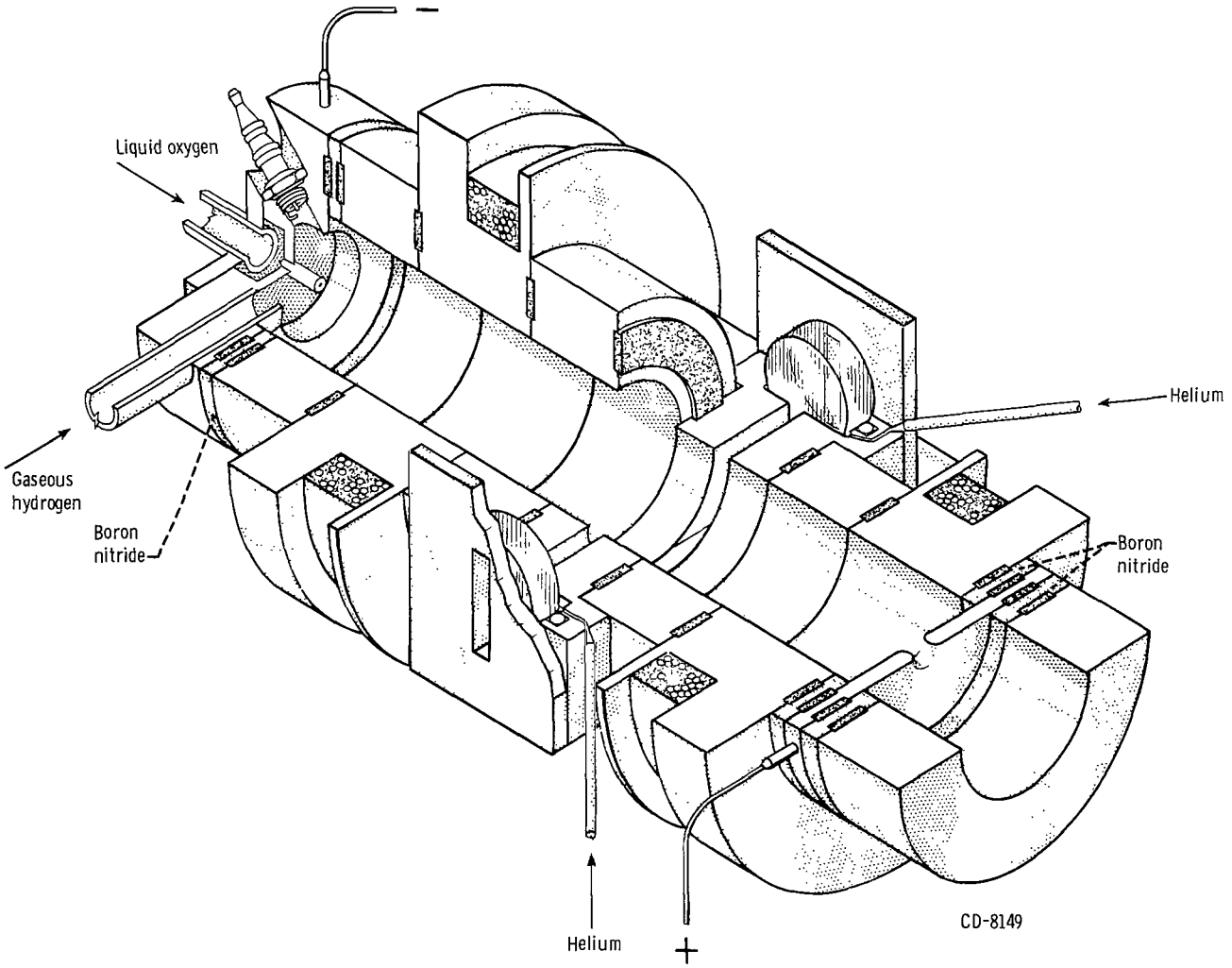

Figure 2. - Gaseous-hydrogen - liquid-oxygen combustor. Single jet injector diameter for oxygen, 0.100 inch; chamber length from injector to nozzle, 11.3 inches; chamber diameter, 2.0 inches; nozzle diameter, 0.630 inch.

made of copper, except for electrical insulators. Nylon pipe connectors insulated the combustor electrically from all external liquid- and gas-supply lines. Silicon rubber O-rings provided pressure seals between adjacent combustor sections.

The injector consisted of a single jet 0.100 inch in diameter alined to inject a stream of liquid oxygen down the cylindrical axis of the combustor. This jet was surrounded by a parallel injected flow of gaseous hydrogen. A 600-volt electric potential placed between the injector and the nozzle provided an electric current discharge along the burning jet for the purpose of increasing the ion population in the hot gases. The injector was made the cathode and the nozzle, the anode. Current flowing in the jet was monitored by recording the voltage drop across a 1-ohm series resistor.

Two magnetic coil windings, each consisting of 100 turns of number 14 copper magnet wire, produced a magnetic field parallel to the axis of the combustor. These were wound on 4-inch outside diameter copper engine sections. The width of each winding was 5/8 inch, and the coil ends were separated on the combustor by $5\frac{1}{4}$ inches. Each winding was powered by 30.0-amperes direct current supplied from two 12-volt storage batteries connected in series. This provided a (measured) magnetic field on the chamber axis which varied from 0.0200 weber per square meter halfway between the coils to 0.0380±0.0005 weber per square meter in the plane of the coils.

A 2- by 1/4-inch viewing port equipped with quartz windows provided a cross-sectional view of the 2-inch-diameter chamber at right angles to the chamber axis. This port was placed halfway between the magnet coils where the magnetic field had an intensity of 0.0200 weber per square meter. A helium purge was used to keep the recessed ports and windows free from obstruction by absorbing gases and solid particles resulting from erosion of combustor surfaces.

Radiation from the viewing port was focused on the slit of a grating spectrograph operating in the spectral range of 2500 to 4500 angstroms in the first order. The 2-inch length of the port was focused parallel to the slit of the spectrograph so that long spectral lines were produced (fig. 3) with points along their lengths corresponding to points on the viewing cross section of the combustion chamber. The slit width was set at 30 microns. This technique provided a means of simultaneously studying effects on the spreading of the burning oxygen jet and the emission spectra associated with the combustion. Films were processed and spectral intensity data obtained by methods discussed in reference 2.

The combustor was operated at an oxidant-fuel-weight ratio (o/f) of 3.88 with a maximum deviation from this value of 0.07 for any single run. The average total weight flow for all runs was 0.549 pound per second with a maximum deviation for any single run of 0.007 pound per second. A chamber pressure of 14.0 atmospheres was maintained to within 0.1 atmosphere on all runs. All electrical sources were turned on and the spectrograph slit opened before the start of the combustion, which was 3 seconds in duration.

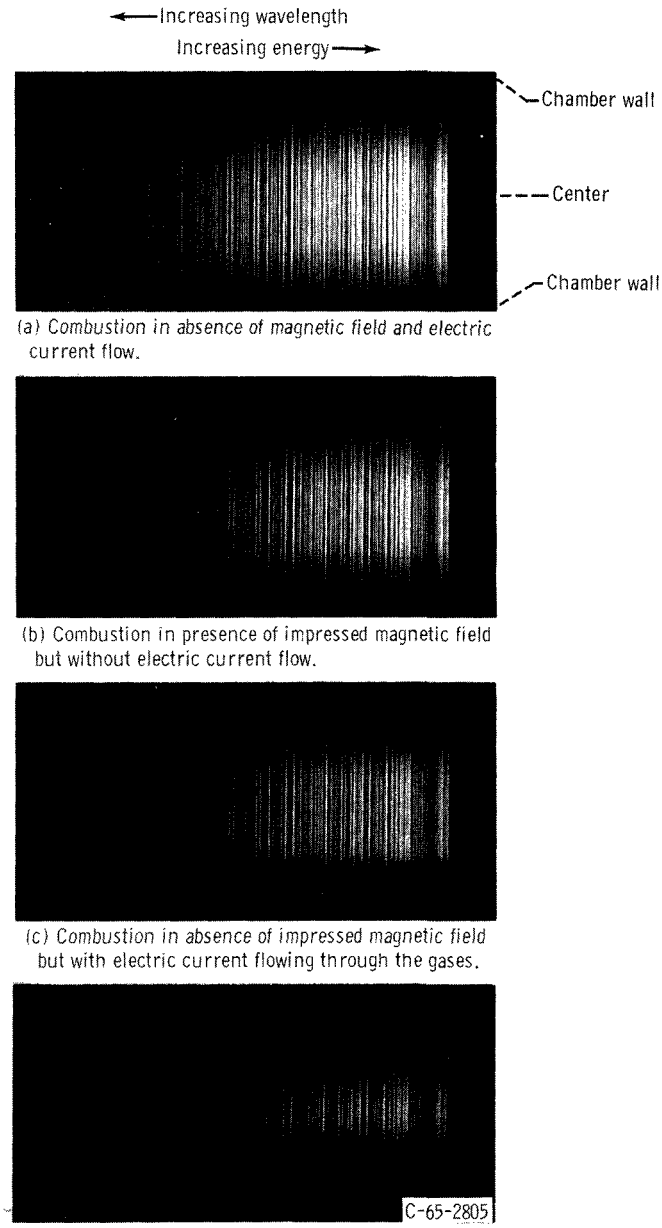

(a) Combustion in absence of magnetic field and electric current flow.

(b) Combustion in presence of impressed magnetic field but without electric current flow.

(c) Combustion in absence of impressed magnetic field but with electric current flowing through the gases.

(d) Combustion in presence of both impressed magnetic field and electric current flow in the gases.

Figure 3. - Hydroxyl radical spectra showing extent of spreading at viewing position of burning oxygen jet (band head at 3064 Å).

With these conditions four types of experiments were carried out (hereinafter referred to as experiments a, b, c, and d, respectively). These were (a) control runs consisting of the combustion in the absence of impressed fields and electric current flow; (b) combustion in the presence of a magnetic field but without electric current flow in the burning jet; (c) combustion in the absence of a magnetic field but with electric current flow produced by the 600-volt applied potential; (d) combustion in the presence of both a magnetic field and electric current flow.

EXPERIMENTAL RESULTS

Spectra

A typical set of spectra corresponding to experiments (a) to (d) is shown in figure 3. The predominant feature is the molecular band head of the (O, O) branch in the $^2\Sigma \rightarrow {}^2\Pi$ electronic transition of the OH radical, which occurs at 3064 angstroms. Other vibrational branches for this transition, including (1, O) and (O, 1), were present on the films but were too weak to show up in the prints. The qualitative nature of the radiation remained the same throughout all the experiments. In general, effects of self-absorption, broadening, background, and overlapping spectra of other molecular bands besides those due to OH were obtained as in previous radiation studies

(ref. 2). Difficulties presented by these interferences were such that no attempt was made to interpret the details of rotational fine structure. A comparison of the general intensity levels of the (O, O), (1, O), and (O, 1) vibrational branches in OH indicated that the (O, 1) intensity may have increased relative to the others whenever an electric current was flowing in the gases. (Within the limits of experimental error the (1, O) and (O, O) intensity levels, as photographically recorded, remained the same from film to film.) However, this effect was difficult to distinguish because of the many errors involved in comparing photographic spectral intensities over the required wavelength intervals. Consequently, while relative vibrational intensity changes in the OH radiation would not be surprising, little confidence or importance was placed on such changes in this work, and their investigation was considered outside the scope of the present report.

Electrical Properties of Burning Jet

Whenever the 600-volt potential was placed between the injector and the nozzle, a current flow that varied erratically between 30 and 200 milliamperes was obtained during the entire duration of combustion. The existence of actual magnetic forces on the flow stream (as is evident from the data given in the section Electromagnetic Effects on Flow Stream) established that the current was flowing through the combustion gases and could not be attributed to a leakage path by way of the copper walls of the combustor. On the basis of Ohm's law, the observed currents corresponded to an overall electrical resistance of the burning jet of 3000 to 20 000 ohms. The lower value corresponded to rather peaked current surges during the combustion and indicated tendencies toward momentary high degrees of electrical breakdown.

Electromagnetic Effects on Flow Stream

The extent of spreading of the combustion zones in experiments (a) to (d) (as indicated by the emitted radiation) is shown in figures 3 and 4. In figure 4 the fraction of maximum intensity I/I_{max} of the (O, O) band head of OH for each spectrum of figure 3 was plotted against position on the chamber cross section. Figures 4(b) and (c) show a slight narrowing when a magnetic field or electric current was applied separately. However, figure 4(d) shows that a marked narrowing occurred when a combination of these two influences was applied. In this case the combustion zone was contracted to about one-half of that obtained with no external influences. (A few runs were made where the discharge did not exceed 150 mÅ because of film deposition on the nozzle. In such instances the magnitude of the constriction was somewhat reduced.)

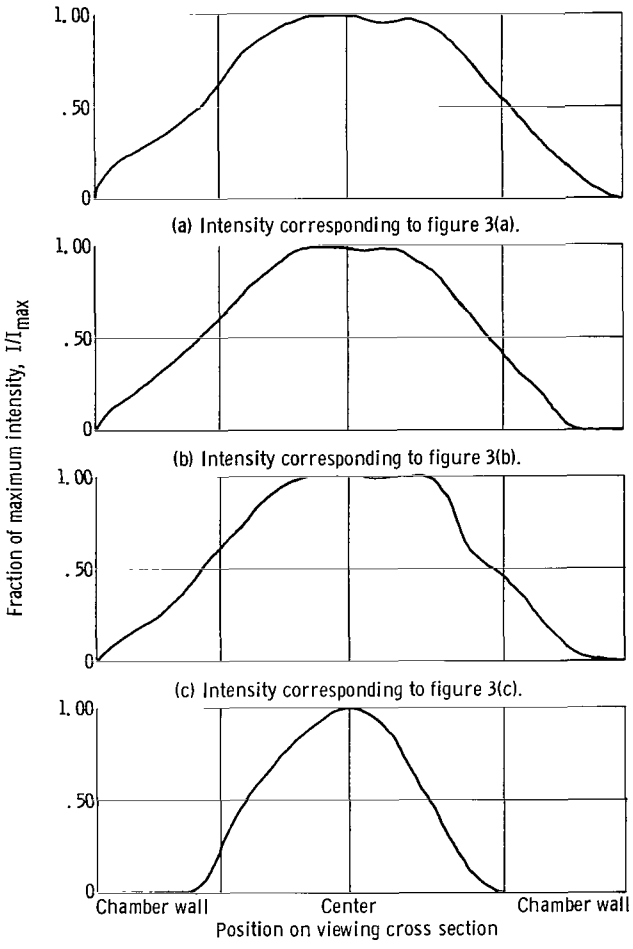

Figure 4. - Intensity of ultraviolet OH emission across viewing cross section.

DISCUSSION

The results shown in figure 4 indicate that magnetic control of the directional flow of combustion gases in hydrogen-oxygen combustion at 14.0 atmospheres pressure can be achieved provided that a sufficiently high ion population and electrical conductivity can be maintained. It appears that in the combustion system with only the magnetic field applied these conditions might not be realized.

Two simple techniques that can be used for increasing the ion population in a hot gas are seeding and the application of an electric discharge. Seeding increases the thermal ion population by adding atomic and molecular species with relatively low ionization potentials to the system. If this technique is used, one must choose a seeding material with a low ionization potential, and also one that will not react chemically to form molecular species with high dissociation energies. Such occurrence would defeat the aim of reducing the ionization potential of the system. Consequently, the method of seeding requires a consideration of the chemistry of each individual combustion system. Table I is a summary of thermal ion populations calculated for three ionization potentials by assuming the validity of the Saha equation (ref. 3, p. 92) and the ideal gas law. From this table it is seen how the ion population changes with ionization potential, temperature, and pressure, and that the above conclusion about the ion population in the combustion system, taken by itself, might be expected for the temperature range of interest (3000° to 4000° K).

In this work a need for any detailed chemical considerations has been avoided by passing an electric discharge through the gases. This technique increased the ion population and electrical conductivity by producing and sustaining a state of electric breakdown in the gases. The ion population and conductivity produced were sufficient to permit a magnetic deflection of the flow stream. In particular it should be noted that the electrical currents and magnetic field strengths needed to produce this effect were not

TABLE I. - TOTAL THERMAL ION POPULATIONS FOR SINGLY CHARGED IONS

$[M \rightleftharpoons M^+ + e^-.]$

Temperature, °K	Ion population, [a] N_o, ions/m^3							
	Pressure, P, atm							
	1	10	20	30	40	50	60	70
Ionization potential for hydrogen-oxygen combustion, [b] v_i, 12.5								
1 000	1.3×10^{-6}	4.1×10^{-6}	5.9×10^{-6}	7.0×10^{-6}	8.2×10^{-6}	8.8×10^{-6}	9.7×10^{-6}	10×10^{-6}
2 000	0.95×10^{10}	2.9×10^{10}	4.1×10^{10}	5.1×10^{10}	5.9×10^{10}	6.6×10^{10}	7.0×10^{10}	7.7×10^{10}
3 000	1.8×10^{15}	5.9×10^{15}	8.3×10^{15}	10×10^{15}	11×10^{15}	13×10^{15}	14×10^{15}	15×10^{15}
4 000	0.84×10^{18}	2.6×10^{18}	3.7×10^{18}	4.6×10^{18}	5.3×10^{18}	5.9×10^{18}	6.4×10^{18}	6.9×10^{18}
5 000	0.35×10^{20}	1.1×10^{20}	1.5×10^{20}	1.9×10^{20}	2.2×10^{20}	2.5×10^{20}	2.6×10^{20}	2.9×10^{20}
6 000	0.39×10^{21}	1.3×10^{21}	1.8×10^{21}	2.2×10^{21}	2.5×10^{21}	2.8×10^{21}	3.1×10^{21}	3.4×10^{21}
7 000	0.23×10^{22}	0.73×10^{22}	1.0×10^{22}	1.2×10^{22}	1.4×10^{22}	1.6×10^{22}	1.8×10^{22}	1.9×10^{22}
8 000	0.88×10^{22}	2.8×10^{22}	4.0×10^{22}	4.8×10^{22}	5.6×10^{22}	6.2×10^{22}	6.8×10^{22}	7.3×10^{22}
9 000	0.24×10^{23}	0.80×10^{23}	1.1×10^{23}	1.4×10^{23}	1.6×10^{23}	1.8×10^{23}	2.0×10^{23}	2.0×10^{23}
10 000	0.59×10^{23}	1.9×10^{23}	2.6×10^{23}	3.2×10^{23}	3.7×10^{23}	4.1×10^{23}	5.0×10^{23}	4.9×10^{23}
Intermediate ionization potential, v_i, 6								
1 000	0.32×10^{11}	1.0×10^{11}	1.5×10^{11}	1.8×10^{11}	2.0×10^{11}	2.3×10^{11}	2.5×10^{11}	2.8×10^{11}
2 000	1.5×10^{18}	4.6×10^{18}	6.6×10^{18}	7.9×10^{18}	9.4×10^{18}	10×10^{18}	11×10^{18}	12×10^{18}
3 000	0.54×10^{21}	1.7×10^{21}	2.4×10^{21}	3.1×10^{21}	3.5×10^{21}	3.9×10^{21}	4.1×10^{21}	4.4×10^{21}
4 000	1.1×10^{22}	3.4×10^{22}	4.8×10^{22}	5.8×10^{22}	6.8×10^{22}	7.5×10^{22}	8.1×10^{22}	9.0×10^{22}
5 000	0.64×10^{23}	2.0×10^{23}	2.9×10^{23}	3.5×10^{23}	4.0×10^{23}	4.6×10^{23}	4.9×10^{23}	5.3×10^{23}
6 000	0.23×10^{24}	0.69×10^{24}	0.98×10^{24}	1.2×10^{24}	1.4×10^{24}	1.6×10^{24}	1.8×10^{24}	1.9×10^{24}
7 000	0.50×10^{24}	1.7×10^{24}	2.3×10^{24}	2.8×10^{24}	3.3×10^{24}	3.7×10^{24}	4.0×10^{24}	4.2×10^{24}
8 000	0.99×10^{24}	3.1×10^{24}	4.4×10^{24}	5.4×10^{24}	6.2×10^{24}	7.0×10^{24}	7.6×10^{24}	8.2×10^{24}
9 000	1.2×10^{24}	4.9×10^{24}	7.2×10^{24}	8.8×10^{24}	10×10^{24}	11×10^{24}	13×10^{24}	14×10^{24}
10 000	0.13×10^{25}	0.70×10^{25}	1.0×10^{25}	1.3×10^{25}	1.5×10^{25}	1.8×10^{25}	1.9×10^{25}	2.2×10^{25}
Ionization potential for pure cesium gas, v_i, 3.87								
1 000	0.79×10^{16}	2.5×10^{16}	3.5×10^{16}	4.3×10^{16}	5.0×10^{16}	5.6×10^{16}	6.1×10^{16}	6.6×10^{16}
2 000	0.72×10^{21}	2.3×10^{21}	3.2×10^{21}	4.0×10^{21}	4.4×10^{21}	5.1×10^{21}	5.7×10^{21}	6.2×10^{21}
3 000	0.34×10^{23}	1.1×10^{23}	1.6×10^{23}	1.9×10^{23}	2.2×10^{23}	2.4×10^{23}	2.6×10^{23}	2.8×10^{23}
4 000	0.24×10^{24}	0.73×10^{24}	1.0×10^{24}	1.3×10^{24}	1.5×10^{24}	1.6×10^{24}	1.8×10^{24}	2.0×10^{24}
5 000	0.76×10^{24}	2.4×10^{24}	3.5×10^{24}	4.2×10^{24}	4.8×10^{24}	5.4×10^{24}	5.8×10^{24}	6.6×10^{24}
6 000	1.8×10^{24}	5.4×10^{24}	7.8×10^{24}	9.5×10^{24}	11×10^{24}	12×10^{24}	13×10^{24}	14×10^{24}
7 000	0.17×10^{25}	0.86×10^{25}	1.2×10^{25}	1.6×10^{25}	1.8×10^{25}	2.1×10^{25}	2.3×10^{25}	2.5×10^{25}
8 000	0.17×10^{25}	1.1×10^{25}	1.8×10^{25}	2.3×10^{25}	2.7×10^{25}	3.0×10^{25}	3.4×10^{25}	3.8×10^{25}
9 000	0.16×10^{25}	1.3×10^{25}	2.2×10^{25}	2.9×10^{25}	3.4×10^{25}	4.0×10^{25}	4.5×10^{25}	4.9×10^{25}
10 000	0.14×10^{25}	1.3×10^{25}	2.3×10^{25}	3.2×10^{25}	4.0×10^{25}	4.7×10^{25}	5.4×10^{25}	6.0×10^{25}

[a] Ion population is $N_o = 2\left(\frac{1}{R}\frac{P}{T}\right)\eta x$ where $\log\left[x^2/(1-x^2)\right]P = (-5050\ v_i/T) + 2.5 \log T - 6.5$.

[b] Estimated from table 4.4, ref. 3, p. 83.

unduly high. On the basis of total weight flow, the electric current flow in the gases amounted to 0.055 to 0.36 coulomb per pound, or in terms of power, 33 to 220 watt-seconds per pound. The influence of these currents can be seen by considering the fluid system in terms of its classification as a plasma. According to accepted usage (ref. 4, p. 272), a fluid can be classified as a plasma if $L \gg h$, where L is the characteristic length of a volume element of fluid Q and h is the Debye shielding length given by

$$h = \left(\frac{\epsilon_o kT}{2N_o q^2}\right)^{1/2} = 49.2\left(\frac{T}{N_o}\right)^{1/2} \quad \text{(meters)}$$

The last expression gives h in meters if T is in degrees Kelvin and N_o is in ions per cubic meter. (All symbols are defined in appendix B.) For our purposes, this quantity serves as a criterion distinguishing macroscopic systems (which can be treated by methods of macroscopic fluid mechanics) from those requiring a more detailed "microscopic" treatment. From table I, it is seen that if one relied only on thermal ionization to determine the ion population in hydrogen-oxygen combustion, N_o would be about 7×10^{15} ions per cubic meter at 3000° K and about 3×10^{18} ions per cubic meter at 4000° K (for 14.0-atm pressure), which corresponds to a range in h of 3×10^{-5} to 2×10^{-6} meter. On the other hand, it is calculated in appendix A that the electric discharge maintained a minimum ion population of 3×10^{17} ions per cubic meter (assuming a burning temperature range of 3000° to 3500° K), which corresponds to a value for h of 5×10^{-6} meter or less during the combustion.

The present combustor achieved a rather low c* efficiency (ref. 5) of around 50 percent, with a slight lowering (about $1\frac{1}{2}$ percent) observed in experiments of type d. The lowering of c* efficiency was probably due to a reduction in the mixing efficiency in the presence of magnetic confinement. While this result is not surprising for the combustor configuration used, it is of little consequence for this study. The injector system was not chosen for the achievement of high c* efficiencies but rather as an ideal observational system in which magnetic influences on a burning flow system could be studied as depicted in figure 1 (p. 2).

In addition to modifying heat transfer, magnetic forces could likely be used to control the amplitude of hydrodynamic flow oscillations in a combustor by exerting directional damping influences on the flow system.

SUMMARY OF RESULTS

A study of the influence of a magnetic field on the directional flow of hot gases in

hydrogen-oxygen combustion at a pressure of 14.0 atmospheres yielded the following results

1. An applied magnetic field of 0.02 weber per square meter was sufficient to influence flow direction in a combustion flow stream at several atmospheres pressure provided that the gases had a sufficiently high electrical conductivity.

2. Apparently the electrical conductivity required for this influence is higher than that normally existing in hydrogen-oxygen combustion taking place in the temperature range of 3000° to 3500° K at 14.0 atmospheres pressure. However, this can be increased sufficiently by allowing a small electric current discharge to flow in the combustion system.

Lewis Research Center,
National Aeronautics and Space Administration,
Cleveland, Ohio, September 17, 1965.

APPENDIX A

ELECTROMAGNETIC PROPERTIES OF COMBUSTION FLUID SYSTEM

A theoretical consideration of electromagnetic forces that can act on a fluid system involves a study of the equations of magnetic fluid dynamics. For a macroscopic formulation (which will be used) these equations are obtained by combining Maxwell's equations with the equations of fluid dynamics and are discussed in some detail elsewhere (ref. 6, ch. 6; ref. 7, ch. VIII; ref. 4, ch. 14). Other possibilities include microscopic formulations using the principles of kinetic theory. In general, these may be quite complicated, and the physical conditions to be introduced will vary greatly with types of electrical properties, as well as with the nature of fluid motion. There are several factors in the case presented herein which seriously restrict our ability to attempt any detailed theoretical treatment (even in the macroscopic sense). Not the least of these is a lack of quantitative understanding of any but bulk electrical properties of combustion gases undergoing chemical reaction; this lack in turn is coupled with problems of mixing and nonsteady flows in the combustor. Consequently, in this appendix we shall proceed mostly by analogy to an idealized problem that clearly exhibits the physical conditions necessary to achieve magnetic control of flow direction and make certain general observations about the nature of this fluid system.

Consider a volume element of fluid Q with characteristic length L, electrical conductivity σ, and fluid density ρ, moving with velocity $\vec{u}$ in the presence of local electric and magnetic fields $\vec{E}$ and $\vec{B}$, respectively. (The magnetic permeability μ will be taken as 1, thus treating any paramagnetic properties such as those of molecular oxygen as of secondary importance.) The fluid can be considered a conductor if the characteristic electrical relaxation time t_c (ref. 4, p. 140) is small compared with characteristic times of flow fluctuations. (This will be sufficiently good for our purposes if the frequency defined by $\omega = 1/t_c$ is greater than about 1 Mc/sec.)

In general, the motion of a conductor in a magnetic field will cause electric currents to flow, resulting in complex interactions with all electric and magnetic fields that may be present and with the flow itself. The total electric current density $\vec{j}$ in volume element Q is related to the fields $\vec{E}$ and $\vec{B}$ through Ohm's law:

$$\vec{j} = \sigma(\vec{E} + \vec{u} \times \vec{B}) \tag{B1}$$

In addition, the magnetic field is subject to a divergence condition

$$\vec{\nabla} \cdot \vec{B} = 0 \tag{B2}$$

and a time rate of change governed by Faraday's law

$$\vec{\nabla} \times \vec{E} = - \frac{\partial \vec{B}}{\partial t} \tag{B3}$$

while the general fluid motion itself conforms to the equation of continuity

$$\frac{\partial \rho}{\partial t} + \vec{\nabla} \cdot (\rho \vec{u}) = 0 \tag{B4}$$

Now consider the condition where σ is sufficiently large (see following discussion) that

$$\frac{\vec{j}}{\sigma} \to 0 \tag{B5}$$

Then

$$\vec{E} = -\vec{u} \times \vec{B} \qquad \text{or} \quad \vec{\nabla} \times \vec{E} = -\vec{\nabla} \times (\vec{u} \times \vec{B}) \tag{B6}$$

Substituting equation (6) into (3), expanding the result by vector identity, and noting condition (2) give

$$\frac{\partial \vec{B}}{\partial t} = (\vec{B} \cdot \vec{\nabla})\vec{u} - (\vec{u} \cdot \vec{\nabla})\vec{B} - \vec{B}\vec{\nabla} \cdot \vec{u} \tag{B7}$$

Using the condition $\vec{\nabla} \cdot \vec{u} = -(1/\rho)[(\partial \rho / \partial t) - \vec{u} \cdot \vec{\nabla}\rho]$ from equation (4) and noting that the operator $\partial/\partial t + \vec{u} \cdot \vec{\nabla} \equiv D/Dt$ is the "substantial derivative" allows equation (7) to be written as

$$\frac{D}{Dt}\left(\frac{\vec{B}}{\rho}\right) = \left(\frac{1}{\rho}\right)(\vec{B} \cdot \vec{\nabla})\vec{u} \tag{B8}$$

On the other hand, it is easily shown (ref. 7, p. 216) that if $\vec{\ell}$ represents an element of length on a fluid line, its rate of change is given by

$$\frac{D}{Dt}(\vec{\ell}) = (\vec{\ell} \cdot \vec{\nabla})\vec{u} \tag{B9}$$

Consequently, when the conductivity conditions for the derivation of equation (8) hold, both $\vec{B}/\rho$ and $\vec{\ell}$ experience rates of change governed by similar formulas. If, as is

presently the case, an external field $\vec{B}$ is imposed on a reaction chamber prior to the presence of fluids in motion, then to the extent that $\vec{B}$ can remain unaltered upon injection of a conducting fluid, a change in $\vec{\ell}$ must correspond to a change in ρ in the direction of $\vec{B}$.

A point must now be made concerning the application of this derivation that requires a more quantitative view of the fluid system. For this purpose three quantities must be considered: the Reynolds number Re, the magnetic interaction parameter N, and the magnetic Reynolds number Re_m (ref. 6, p. 172). These are given by

$$Re = \frac{uL}{\nu} \tag{B10}$$

where ν represents the kinematic viscosity,

$$N = \frac{\sigma B^2 L}{\rho u} \tag{B11}$$

and

$$Re_m = \mu \sigma u L \tag{B12}$$

The product of equations (10) and (11) defines another quantity, the Hartmann number, given by

$$H^2 = \frac{B^2 L^2 \sigma}{\rho \nu} \tag{B13}$$

and represents a measure of magnetic forces as compared with viscous forces. The magnetic interaction parameter represents the ratio of $\vec{u} \times \vec{B}$ forces to inertial forces, whereas the magnetic Reynolds number measures the distortion that the fluid motion produces on the magnetic field. For magnetic forces to dominate viscous and inertial forces, $H > 1$ and $N > 1$, whereas for the magnetic field to remain unaltered by the flow $Re_m << 1$.

We will now attempt to establish maximum ranges for Re, N, Re_m, and H by taking fluid dimensions to be characterized either by the full chamber length (for the assumption of a completely continuous fluid) or by the dimensions of a small pocket of combustion gases (about 10^{-4} m), with the electrical conditions as deduced from the overall electrical resistance of the combustion system. The pertinent quantities are then obtained as follows:

Viscosity (estimated from ref. 8), kg/sec-m . . . . . 7×10^{-5} to 8×10^{-5}
Average molecular weight (estimated for equilibrium composition at o/f = 3.88), kg/mole . . . . . 1×10^{-2}
Average molar population (from ideal gas law at 14 atm and 3000^{o} to 3500^{o} K), moles/m^3 . . . . . 49.0 to 57.0
Average density, kg/m^3 . . . . . 0.49 to 0.57
Kinematic viscosity (viscosity/density), ν, m^2/sec . . . . . 1.2×10^{-4} to 1.6×10^{-4}
Average weight flow, kg/sec 0.25
Area (1/2 chamber radius to full chamber radius), m^2 . . . . . 2×10^{-3} to 8×10^{-3}
Length (from gas pocket size to full chamber length), m . . . . . 10^{-4} to 0.28
Average velocity (free stream), weight flow/(density)(area), m/sec . . . . . 54 to 250
Conductivity, length/(resistance)(area), (for length, 0.28 m), mho/m . . . . . 1.7×10^{-3} to 4.7×10^{-2}

From these quantities maximum ranges for Re, N, Re_m, and H are obtained:

$$3.4\times10^{1} \leq Re \leq 5.8\times10^{5}$$

$$4.9\times10^{-13} \leq N \leq 2.0\times10^{-7}$$

$$9.2\times10^{-6} \leq Re_m \leq 3.3\times10^{0}$$

$$4.1\times10^{-6} \leq H \leq 3.5\times10^{-1}$$

On the basis of these calculations both the Hartmann number and the magnetic interaction parameter are appreciably less than unity, and hence the magnetic forces cannot dominate the viscous and inertial forces present in the combustor. It is evident that the macroscopic considerations used herein are not adequate for explaining the observed flow constriction caused by the current flow and the applied magnetic field. Valid conclusions cannot be obtained, therefore, from calculations based on free-stream flow conditions and the assumption of fluid continuity. This is particularly the case if electric conductivity is estimated from the electric current drawn by the overall flow stream. In this respect considering "granular structure" in the combustor is necessary. Existing evidence (ref. 2, fig. 8) indicates that the hot luminous portions of a rocket combustion system (as considered here) do not form a completely continuous medium, but that a considerable tendency exists for the overall flow system to be made up of pockets of hot gases. The time-dependent structure of such granulation depends on the jet breakup and mixing conditions prevailing in the combustor and is coupled with the burning itself. Consequently, conclusions regarding local conductivity (and possibly other properties) should

probably not be made on the basis of measurements for the overall volume of reacting gases.

Finally, it is necessary to estimate a lower limit for the ion population produced in the system, which was previously used to determine an upper limit for the Debye shielding length. At the oxidant-fuel weight ratio and chamber pressure used, the following equilibrium composition is estimated (with 100 percent vaporization and burning efficiency assumed) (ref. 8):

Species	Mole fraction
H	0.019
H_2	.49
H_2O	.47
O	.0002
O_2	.00008
OH	.006

When each atom and molecule is assumed to act as a charge carrier, this composition gives 47 equivalents per pound. The present calculation is based on a view of electric current flow that depicts charges being carried in the flow stream by association with molecules. This problem involves overall mass transport and is to be distinguished from current flow between electrodes in a sealed gas-filled tube. The latter is a diffusion problem that is usually treated in terms of a sum-over-charge carriers with specified mean collision times (ref. 4, ch. 7). For currents used here,

$$\left(\frac{1}{96\ 500}\ \frac{\text{faraday}}{\text{C}}\right)\left(0.06 \text{ to } 0.36\ \frac{\text{C}}{\text{lb}}\right) = 6\times10^{-7} \text{ to } 4\times10^{-6} \text{ faraday/lb}$$

With 1 faraday $\longleftrightarrow$ 1 equivalent (with equivalent as used here), 6×10^{-7} to 4×10^{-6} equivalents per pound weight flow served as charge carriers, with only single ionization assumed. Dividing these values by 47 equivalents per pound gives an "effective degree of ionization" during current flow of $x = 1\times10^{-8}$ to 8×10^{-8}. With the temperature range of burning taken as 3000° to 3500° K at a pressure of 14 atmospheres, the ideal gas law gives the concentration of charge carriers as 57.0 moles per cubic meter at 3000° K to 49.0 moles per cubic meter at 3500° K. This concentration gives an ion population of

$$N_o = (\text{moles/m}^3)(6.0\times10^{23} \text{ molecules/mole})(x)(1 \text{ ion/molecule}) = \text{ions/m}^3$$

where

$$N_o = 2.9\times10^{17} \qquad \text{(for } T = 3500^{o} \text{ K; } x = 1\times10^{-8}\text{)}$$

$$= 4.5\times10^{17} \qquad \text{(for } T = 3000^{o} \text{ K; } x = 1\times10^{-8}\text{)}$$

$$= 2.4\times10^{18} \qquad \text{(for } T = 3500^{o} \text{ K; } x = 8\times10^{-8}\text{)}$$

$$= 2.7\times10^{18} \qquad \text{(for } T = 3000^{o} \text{ K; } x = 8\times10^{-8}\text{)}$$

When these ion populations are compared with table I (p. 8), they are seen to be close to thermal ion populations that would require a burning temperature of 4000^{o} K. Since the actual c* efficiency was only around 50 percent, there were fewer equivalents per pound than calculated here. Therefore these values for N_o are probably low and represent only lower limits for the ion population in the hot portions of the combustion system (which are the parts to control). Consequently, the Debye shielding lengths calculated from these values represent maximum lengths for the system considered.

APPENDIX B

SYMBOLS

$\vec{B}$	magnetic induction (mean magnetic field in matter)
C	Coulomb
c*	characteristic exhaust velocity
$\vec{E}$	electric field
H	Hartmann number
h	Debye shielding length
I	radiation intensity
$\vec{j}$	vector electric current density
k	Boltzmann's constant
L	characteristic length of Q
$\vec{\ell}$	vector element of length on a fluid line
M	general designation for atom or molecule
N	magnetic interaction parameter
N_o	ion population
o/f	oxidant-fuel weight ratio
P	pressure
Q	volume element of fluid
q	electric charge
R	universal gas constant, (82.057 $(cm^3)(atm)/(^oK)(mole)$)
Re	Reynolds number
Re_m	magnetic Reynolds number
T	temperature, ^oK
t	time
t_c	characteristic electrical relaxation time in a fluid
$\vec{u}$	vector velocity
v_i	ionization potential
x	degree of ionization
ϵ_o	permittivity of free space
μ	magnetic permeability
η	Avagadro's number
ν	kinematic viscosity
ρ	fluid density
σ	electrical conductivity
ω	frequency defined as $1/t_c$

REFERENCES

1. Calote, H. F.: Electrical Properties of Flames. Third Symposium on Combustion, Flame and Explosion Phenomena, The Williams & Wilkins Co., 1949, pp. 245-253.
2. Burrows, Marshall C.; and Razner, Ronald: Relation of Emitted Ultraviolet Radiation to Combustion of Hydrogen and Oxygen at 20 Atmospheres. NASA TN D-2548, 1964.
3. Cobine, J. D.: Gaseous Conductors. Dover Pub., Inc., 1958.
4. Reitz, J. R.; and Milford, F. J.: Foundations of Electromagnetic Theory. Addison-Wesley Pub. Co., Inc., 1960.
5. Sutton, G. P.: Rocket Propulsion Elements. Second ed., John Wiley & Sons, Inc., 1956.
6. Drummond, J. E.: Plasma Physics. Mc-Graw-Hill Book Co., Inc., 1961.
7. Landau, L. D.; and Lifshitz, E. M.: Electrodynamics of Continuous Media. Addison-Wesley Pub. Co., Inc., 1960.
8. Gordon, Sanford; and McBride, Bonnie J.: Theoretical Performance of Liquid Hydrogen with Liquid Oxygen as a Rocket Propellant. NASA MEMO 5-21-59E, 1959.

"The aeronautical and space activities of the United States shall be conducted so as to contribute . . . to the expansion of human knowledge of phenomena in the atmosphere and space. The Administration shall provide for the widest practicable and appropriate dissemination of information concerning its activities and the results thereof."

—NATIONAL AERONAUTICS AND SPACE ACT OF 1958

NASA SCIENTIFIC AND TECHNICAL PUBLICATIONS

TECHNICAL REPORTS: Scientific and technical information considered important, complete, and a lasting contribution to existing knowledge.

TECHNICAL NOTES: Information less broad in scope but nevertheless of importance as a contribution to existing knowledge.

TECHNICAL MEMORANDUMS: Information receiving limited distribution because of preliminary data, security classification, or other reasons.

CONTRACTOR REPORTS: Technical information generated in connection with a NASA contract or grant and released under NASA auspices.

TECHNICAL TRANSLATIONS: Information published in a foreign language considered to merit NASA distribution in English.

TECHNICAL REPRINTS: Information derived from NASA activities and initially published in the form of journal articles.

SPECIAL PUBLICATIONS: Information derived from or of value to NASA activities but not necessarily reporting the results of individual NASA-programmed scientific efforts. Publications include conference proceedings, monographs, data compilations, handbooks, sourcebooks, and special bibliographies.

Details on the availability of these publications may be obtained from:

SCIENTIFIC AND TECHNICAL INFORMATION DIVISION

NATIONAL AERONAUTICS AND SPACE ADMINISTRATION

Washington, D.C. 20546